Effects of geometric and refractive index disorder on wave propagation in two-dimensional photonic crystals

A. A. Asatryan,[1] P. A. Robinson,[1] L. C. Botten,[2] R. C. McPhedran,[1] N. A. Nicorovici,[1] and C. Martijn de Sterke[1]

[1]*School of Physics, The University of Sydney, New South Wales 2006, Australia*

[2]*School of Mathematical Sciences, University of Technology, Sydney, New South Wales 2007, Australia*

(Received 17 February 2000)

The effects of disorder in the geometry and refractive index on the transmittance of two-dimensional photonic crystals composed of dielectric circular cylinders are considered, including randomness of radii, positions of the cylinder centers, and thickness of each layer of the photonic crystal. The effects of combinations of different types of strong disorder are also considered. The localization and homogenization properties of disordered photonic crystals are investigated. Analytical expressions for the two-dimensional localization length in the form of integrals are presented for both polarizations. It is shown numerically that the slope of the exponential divergence of the localization length in two dimensions is proportional to the inverse of the square of randomness for strong disorder and proportional to the inverse of the randomness for weak disorder. The effective dielectric constants for both polarizations in the case of strong disorder are also found. The transition from localization to homogenization is discussed and the terms responsible for this transition are identified and investigated.

PACS number(s): 41.20.Jb, 42.70.Qs, 71.15.−m

I. INTRODUCTION

First introduced by Yablonovitch [1] and John [2] in 1987, photonic crystals are now a substantial area of research [3–5]. Photonic crystals are materials that prohibit the propagation of light in certain directions for some frequencies. Applications of photonic crystals include fabrication of microscopic lasers [6], photonic crystal-based resonant antennas [7], optical fibers with photonic crystal cores [8], and the marriage of a photonic crystal with a liquid crystal to construct an optical switch that operates by controlling the refractive index of the inclusions [9]. One of the aspects of designing new photonic devices such as those mentioned above is the question of their tolerance [10] to imperfections. This problem is closely related to the question of the effects of disorder on the transmittance properties of photonic crystals. In spite of the importance of this problem, there are only a few papers that consider it. Sigalas *et al.* [11] investigated the effects of disorder on two-dimensional photonic crystals composed of circular cylinders. However, due to computer time constraints, the resolution of their results was low. Recently, Asatryan *et al.* [12] investigated the effects of disorder on the transmittance of two-dimensional photonic crystals composed of circular cylinders, using a highly efficient and accurate method [13–15], and considered the effects of disorder due to randomness of the refractive indices of the cylinders. It was found that the transmittance properties of disordered photonic crystals are reminiscent of the optical absorption spectra of amorphous semiconductors. These studies are also important from the point of view of Anderson localization [16] of photons, as it was suggested by John [17] that the construction of a photonic crystal analogous to an amorphous semiconductor would be a way to achieve localization of light.

Refractive index disorder is not unique and other parameters such as the radii or positions of the cylinders can also be disordered. The aim of this paper is to determine the effects of the different types of disorder on the transmittance properties of two-dimensional photonic crystals made from layers of circular cylinders and investigate numerically and theoretically the Anderson localization of electromagnetic waves in such structures. This work can be viewed as a generalization of our earlier paper [12]. In Sec. II we outline the general physical situation and give the background of the problem. In Sec. III A we briefly review the effects of refractive index disorder on the transmittance as reported earlier [12], to be able to compare it to the other types of disorder considered later in Sec. III. In Sec. III B we consider radius disorder of cylinders, while positional disorder, in which the centers of the cylinders of each layer of the photonic crystal are randomly distributed, is considered in Sec. III C. In this section we consider also ''sliding'' disorder, in which the layers of the photonic crystal are slid randomly relative to each other in the transverse direction (i.e., parallel to the layers themselves). Section III D deals with thickness disorder, in which the thicknesses of the layers are random. In Sec. III E, the effects of a combination of disorders are considered, and the key parameters that have the most effect on the transmittance are determined. The localization of electromagnetic waves and the transition from localization to homogenization for both polarizations are studied in Sec. IV. An analytical expression of the localization length's dependence on the wavelength in the form of a quadrature is also given for each polarization.

II. BACKGROUND

We consider a photonic crystal [12–15], comprising a finite stack of N_L gratings, each of which comprises a set of parallel, periodically repeating cylinders (Fig. 1). The thickness h_L of each grating can be arbitrary, but the period D is the same for all layers. Each period of grating has a set of N_c nonoverlapping circular cylinders. The refractive indices n_l, radii a_l, and positions c_l of the centers of the cylinders can

 ©2000 The American Physical Society

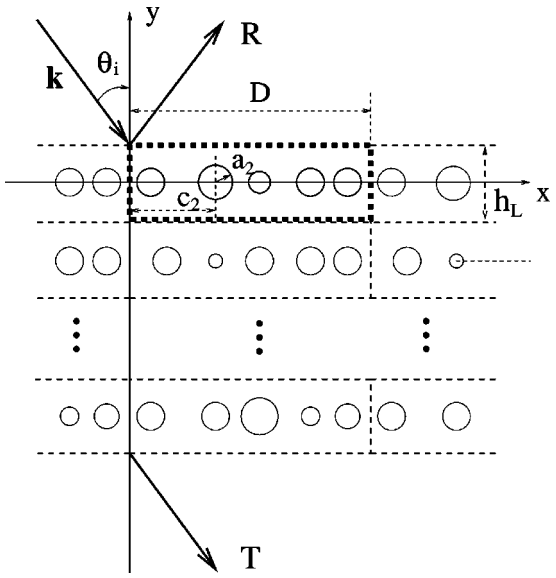

FIG. 1. The geometry of the problem. A plane wave of wave vector **k** is incident at an angle θ_i on a stack of gratings composed of N_c circular cylinders per unit cell (indicated by the heavy dashes) of radii a_i and centers c_i. The period of the grating is D and the separation of the layers is d, which is also the mean cylinder separation. Reflected and transmitted waves are labeled R and T, respectively.

be arbitrary within the unit cell of the grating. In this paper, however, for reasons of computational simplicity and speed, we confine ourselves to the case in which the centers c_l of the cylinders are located on the mid-plane of each layer, so as to have up or down symmetry within the grating (for more details see [13–15]).

A plane wave of wavelength λ is incident in free space at an angle θ_i on this structure (see Fig. 1). Here we confine ourselves to the case of in-plane incidence in which the wave vector **k** lies in the xy plane (Fig. 1). In this case, the polarizations of the field decouple and the problem can be specified by a single component V: $V=E_z$ when the electric vector is along the cylinder axes and $V=H_z$ when the magnetic vector is along these axes of the cylinders.

The method developed in [13–15] provides a highly efficient way to calculate the transmittance T and the reflectance R of the structure described above, whether in single reflected and transmitted orders at longer wavelengths, or in multiple orders at shorter wavelengths. The solution is found in two steps. First we calculate the reflection **R** and transmission **T** matrices for each grating, then the transmittance of the entire stack is found using an inductive treatment [13–15]. The method allows us to consider cases in which the cylinders are close to touching, though interpenetration of layers is not allowed.

III. EFFECTS OF DISORDER ON THE TRANSMITTANCE

In this section we consider the effects of different types of disorder on the transmittance properties of a photonic crystal for normal plane wave incidence, $\theta_i=0$. Before disordering all parameters at once in Sec. III E, we first consider the effects of the different types separately. The effects of the disorder are investigated via the changes they produce in the average of the logarithm of the transmittance $\langle \ln T \rangle$ compared to $\ln T$ for an ordered photonic crystal. We choose the quantity $\langle \ln T \rangle$ as an indicator of the effects of disorder because it determines the localization length (see Sec. IV A), it is a self averaging quantity [18], and it is sensitive to the disorder over a large range of wavelengths.

The random parameter ξ is set as

$$\xi=\bar{\xi}+\delta\xi, \tag{1}$$

where $\bar{\xi}$ is the regular part of ξ, and $\delta\xi$ is a random variable uniformly distributed in the range $[-Q_\xi, Q_\xi]$. Here ξ can represent the refractive index n_l, radius a_l, position c_l of the center of the cylinders, the layer thickness h_L, or the transverse sliding distance s_L. By changing the value of Q_ξ we can investigate the effects of different degrees of disorder on $\langle \ln T \rangle$ as a function of wavelength λ. By strong disorder we mean disorder in which the variation of the random parameter is comparable to its mean.

In the numerical calculations throughout this paper, we choose the period of the grating to be $D=10d$, with $N_c=10$ cylinders per unit cell, where d is the mean separation between cylinders. In the absence of disorder ($Q_\xi=0$), the cylinders are equally spaced by $d_x=D/10=d$ and form a square lattice $h_L=d_x=d$. The average refractive index of the cylinders is $\bar{n}=3.0$, while the average radius of the cylinders preserves the filling fraction $\bar{f}=\pi\bar{a}^2/d^2=0.2827$, so that when $Q_a=0$, $\bar{a}=0.3d$. There are $N_L=20$ layers in the stack and the averaging of $\langle \ln T \rangle$ was carried out over enough realizations of the stack to make the standard error in the mean of the logarithm of the transmittance less then 5% with a maximum of 100 realizations in all cases. The parameters of the calculations were chosen to have the fractional relative accuracy of the transmittance T of each individual realization of the stack better than 10^{-4}.

A. Refractive index disorder

Photonic crystals have band structures analogous to those of semiconductors, with bands of propagating states, separated by band gaps. In the photonic case, the bands and gaps correspond to high and low transmittance, respectively. In band gaps, the density of states, which is the number of propagating modes per unit frequency, vanishes in the limit of an infinite medium. In [12] we reported the effects on the transmittance for refractive index disorder only. The parameters in this previous work were the same as they are here, except that $N_c=5$. We considered the effects of different strengths of refractive index disorder Q_n on the band structure and observed that disorder introduces states into gaps. This is similar to impurity states in doped semiconductors in the gap between the valence and conduction bands. For E_z polarization we found that even a small degree of disorder narrows the first gap significantly from the long wavelength side.

To determine the dependence on N_c we did calculations for $N_c=5$, $N_c=10$, and $N_c=20$ at $Q_n=0.2$. We found that the gap narrows slightly from the long wavelength side but rapidly approaches a limiting form. It was also seen that $\langle \ln T \rangle$ develops tail-like behavior at the long wavelength

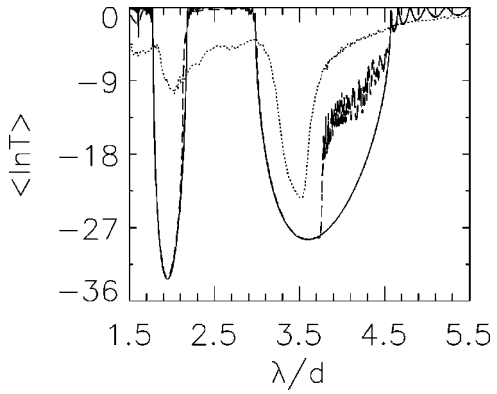

FIG. 2. Plot of $\langle \ln T \rangle$ versus wavelength for E_z polarization for $Q=0$ (solid), $Q_a=0.01d$ (dashed), and $Q_a=0.08d$ (dotted). Other parameters are given in the text.

edges of the gaps [12]. From our calculations we conclude that $N_c=5$ cylinders per unit cell is sufficient to describe the effects of disorder, at least semiquantitatively; nonetheless, throughout this paper $N_c=10$.

B. Radius disorder

In this section we consider the effects of radius disorder on transmittance $\langle \ln T \rangle$ as a function of wavelength. In Fig. 2 we plot $\langle \ln T \rangle$ as a function of wavelength for disorder, with $Q_a=0$, $0.01d$, and $0.08d$ for E_z polarization. The solid line corresponds to $Q_a=0$, when we have no randomness. The band structure has two gaps for wavelengths greater than $1.5d$. The first gap (counting from the right) is at wavelengths $\lambda \approx 3d-5d$ and the second is at $\lambda \approx 1.9d-2.1d$. As is seen in Fig. 2, randomness with $Q_a=0.01d$ (dashed line) affects $\langle \ln T \rangle$ compared with the regular structure (solid line) noticeably more in the first gap than the second. The disorder induces resonances at wavelengths between $3.8d<\lambda<4.5d$ in the first gap, while the second gap is almost unaffected.

As we increase the disorder to $Q_a=0.08d$ (dotted line), the second gap is substantially affected. The quantity $\langle \ln T \rangle$ is increased in the gaps compared to $Q_a=0.01d$, while in the regions between the gaps at wavelengths $2.1d<\lambda<2.95d$, $1.5d<\lambda<1.85d$, and $4.7d<\lambda<5.5d$, $\langle \ln T \rangle$ is decreased. For disorders $Q_a>0.04d$, $\langle \ln T \rangle$ develops tail-like behavior reminiscent of Urbach tails [19]. This behavior of $\langle \ln T \rangle$ is similar to refractive index disorder [12], though the resonances induced in the first gap for refractive index disorder are less pronounced.

We also studied the same dependencies as in Fig. 2, but for $N_c=5$ cylinders per unit cell. We then observe that the resonances induced in the first gap are more pronounced. As we decrease the number of layers N_L in the stack to $N_L=10$ for $N_c=5$ or $N_c=10$, we observe that the number of the resonances decreases. Thus we conclude that this resonance behavior is a whole-stack effect, which involves reflections off front and back interfaces. As the number of layers $N_L \to \infty$, the gaps deepen and the resonances are less prominent.

Figure 3 is similar to Fig. 2, but for H_z polarization. The solid curve corresponds to an ordered photonic crystal with $Q_a=0$. The structure develops two gaps for wavelengths greater than $1.35d$. The first gap, which is very weak for

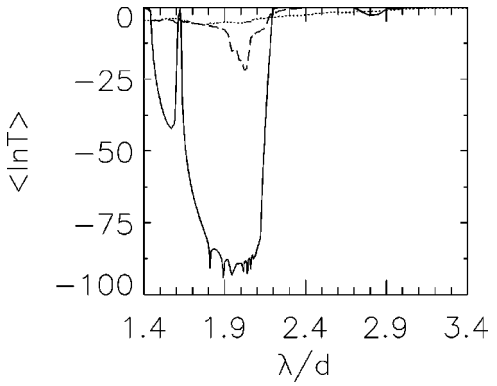

FIG. 3. Same as in Fig. 2, but for H_z polarization.

$N_L=20$, is at $\lambda \approx 2.7d-3d$, while the second gap is at $\lambda \approx 1.4d-2.2d$. The second gap has two parts separated by a narrow band at $\lambda \approx 1.62d$. The disorder $Q_a=0.01d$ has a strong effect on the second gap, and very little effect on the first weak gap. This behavior of $\langle \ln T \rangle$ is similar to refractive index disorder [12]. Disorder with $Q_a=0.08d$ (dotted line) has a very strong effect on the band structure: the band gaps fill in and their locations become indistinct.

C. Positional disorder

Here we consider the effects of positional disorder, restricting attention to gratings in which the centers of the cylinders all have a common value $y=y_L$. The position of the center of a given cylinder c_l is randomly distributed according to Eq. (1) along the line $y=y_L$, subject to the cylinders not overlapping one another. In Fig. 4 we present $\langle \ln T \rangle$ as a function of wavelength for different amounts of disorder Q_c. The solid line corresponds to $Q_c=0$, while the dashed line corresponds to $Q_c=0.05d$. As we see, disorder with $Q_c=0.05d$ has little effect on the second gap, but induces ''resonances'' in the long wavelength part of the first gap. This is similar to radius disorder with $Q_a=0.01d$ (Fig. 2). As we increase the disorder to $Q_c=0.15d$ (dotted line in Fig. 4) the resonances increase their amplitude, but in contrast to the radius disorder case, the gaps become slightly deeper. In studies in course, we have seen that these resonances in the gap can be viewed as being associated with the

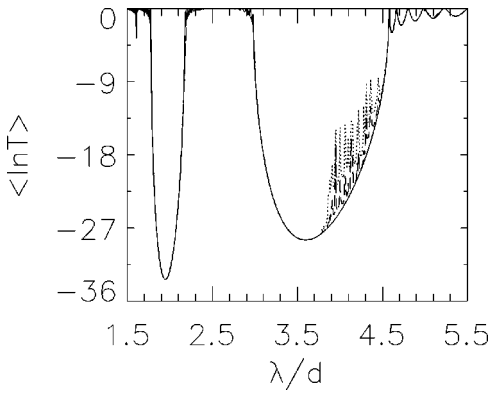

FIG. 4. Plot of $\langle \ln T \rangle$ versus wavelength for E_z polarization for $Q_c=0$ (solid), $Q_c=0.05d$ (dashed), $Q_c=0.15d$ (dotted). There are $N_c=10$ cylinders per unit cell and $N_L=20$ layers in the stack. Other parameters are given in the text.

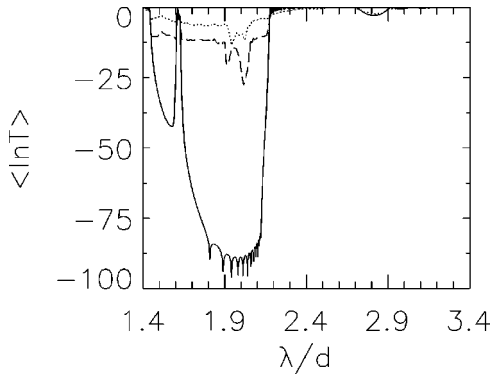

FIG. 5. Same as in Fig. 4, but for H_z polarization.

photonic bands in square arrays of period $2d$, $3d$, etc. The quantity $\langle \ln T \rangle$ decreases in the regions of the pass bands as well. The randomness $Q=0.15d$ has little effect on the second gap, in contrast to radius disorder (see Sec. III B).

Figure 5 is similar to Fig. 4, but for H_z polarization. The overall behavior is now similar to the corresponding radius disorder case, though the randomness has little effect on the first weak gap at $\lambda \approx 2.7d-3d$. The sharp transmission peak at $\lambda=1.62d$ has vanished due to the disorder. Thus the H_z polarization case is much more sensitive to positional disorder than E_z polarization. Even small disordering of the centers of the cylinders ($Q_c=0.05d$) greatly reduces the depth of the second gap. A possible explanation is that for H_z polarization the fields tend to concentrate in the background medium [4], and it is thus sensitive to the randomization of positions. Note that there is not a full gap for this polarization and therefore it is ''easier'' for the incident wave to couple to the modes of a disordered photonic crystal. It has been known since the work of Wood [20] that the properties of diffraction gratings are much more sensitive to profile variations for H_z polarization than for E_z polarization.

We also consider the effects of sliding disorder on $\langle \ln T \rangle$, with each layer being displaced randomly by an amount s_L in the transverse direction. The reason for considering this type of disorder is that the scattering matrices are all identical apart from the phase factor $\exp(iks_L)$, considerably reducing the computation time. As we introduce sliding disorder, the gaps slowly deepen and a narrow gaplike feature develops at $\lambda \approx 1.7d$ for E_z polarization. For H_z polarization we found that the sliding disorder smears out the oscillations of $\langle \ln T \rangle$ at $\lambda \approx 1.9d-2.1d$ near the bottom of the second gap (as in Fig. 3) and slightly deepens the gap. The narrow high transmittance band at $\lambda=1.62d$ is slightly smeared out as well, while disorder has little effect on the first ''weak'' gap. We thus conclude that sliding disorder has stronger effects on H_z polarization than on E_z polarization.

D. Thickness disorder

Here we consider the effects of thickness disorder. The thickness of each layer of the stack is random, with the average thickness $\overline{h_L}=1$. In Fig. 6 we plot $\langle \ln T \rangle$ as a function of wavelength for E_z polarization and for different values of Q_d. The solid line corresponds to $Q_d=0$ and the dashed line to $Q_d=0.1d$. From Fig. 6 we see that thickness disorder smooths the edges of both gaps while their depths decrease.

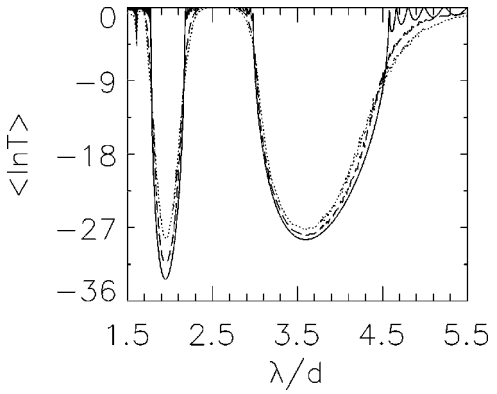

FIG. 6. Plot of $\langle \ln T \rangle$ versus wavelength for E_z polarization for $Q_d=0$ (solid), $Q_d=0.1d$ (dashed), $Q_d=0.15d$ (dotted). There are $N_L=10$ layers in the stack. Other parameters are given in the text.

The oscillations of $\langle \ln T \rangle$ in the vicinity of the edges of the gaps are smeared out by disorder. As we increase the disorder to $Q_d=0.15d$ (dotted line), both gaps become wider and diminish slightly in depth. The number of oscillations near the edges of the gaps are determined by the number of the layers in the stack N_L, and as we increase the thickness disorder we destroy the coherence between the multiply reflected waves in the stack, thereby leading to this ''smoothing'' effect.

Figure 7 is similar to Fig. 6, but for H_z polarization. The solid line corresponds to the ordered photonic crystal $Q_d=0$. For $Q_d=0.1d$, the edges of the gap again become smooth. The gap becomes slightly wider and some of the oscillations in the gap are smeared out. The very narrow transmission band at $\lambda \approx 1.62d$ vanishes due to the disorder. As we increase the disorder to $Q_d=0.15d$, the gap becomes slightly wider and deeper. The randomness has little effect on the first weak gap at $\lambda \approx 2.7d-3d$. The effects of thickness disorder on $\langle \ln T \rangle$ are greater for E_z polarization than for H_z polarization.

E. Effects of a combination of different types of strong disorder

Here we examine the combined effects of the different types of strong disorder. As we have seen in Sec. III there are five parameters that can be disordered: refractive indices n_l, radii a_l, positions c_l, thicknesses h_L, and sliding parameters s_L. The aim here is to find the combinations of disorder

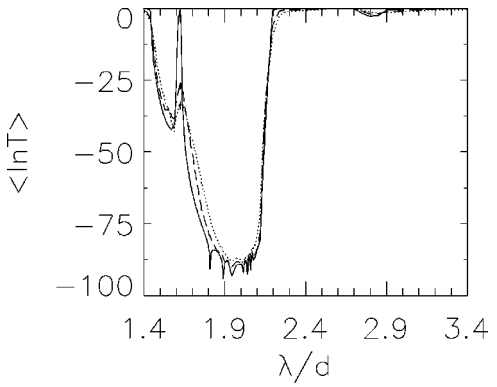

FIG. 7. Same as in Fig. 6, but for H_z polarization.

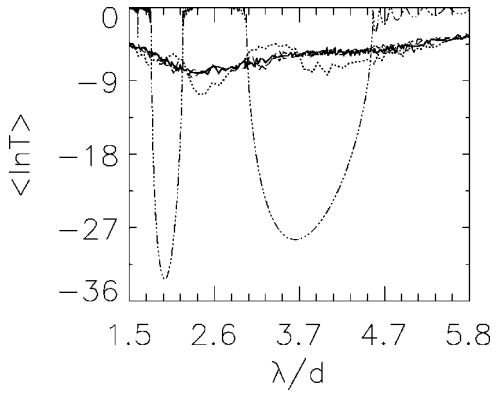

FIG. 8. Combination of strong disorder for E_z polarization. Dashed triple dotted line represents the case of no disorder, the solid line corresponds to all parameters disordered at once, the long dashed line represents refractive index, radius, thickness, and sliding disorder, while the short dashed line is for refractive index and radius disorder only. The dotted line represents the refractive index and thickness disorder. There are $N_c=10$ cylinders per unit cell and $N_L=20$ layers in the stack.

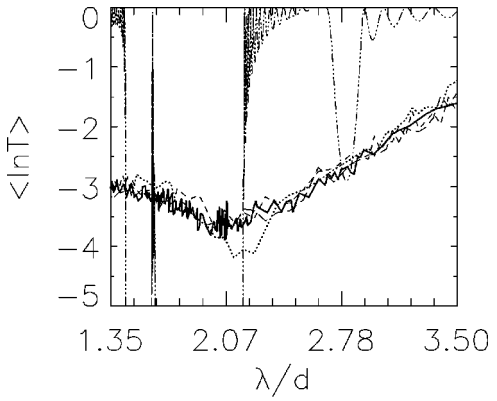

FIG. 9. Same as in Fig. 8, but for H_z polarization.

that have the most effect on $\langle \ln T \rangle$. We first consider all types of disorder simultaneously, then we ''switch them off'' one by one, then pair by pair, and so on, to determine the most influential combinations of disorder. We are constrained in the amount of disorder when we disorder radii, positions, and thicknesses simultaneously because we must avoid the cylinders overlapping.

From our calculations we conclude that refractive index disorder n_l and radius disorder a_l have the most influence on $\langle \ln T \rangle$ for our parameters by considering the strong disorder. In Fig. 8 we present the dependence of $\langle \ln T \rangle$ versus wavelength for E_z polarization, for a combination of strong disorders in which the refractive indices n_l, radii a_l and positions c_l of the cylinders and the thicknesses of the layers h_L are random. The layers are also randomly slid in the transverse direction. The degrees of disorder of the refractive indices, radii, centers of cylinders, thicknesses, and sliding parameters s_L of layers are given by $Q_n=1.5$, $Q_a=0.1d$, $Q_c=0.07$, $Q_h=0.05d$, $Q_s=0.5d$, respectively. As can be seen, the overall effect (solid line in Fig. 8) of the combined disorders is achieved in the presence of just the refractive index and radius disorder, whereas radius or refractive index disorder alone or in combination with position, sliding, and thickness disorders, is not sufficient. Such strong disorder has a pronounced effect on the band structure and the gaps are filled in by combinations of strong disorder.

Figure 9 represents the same cases as in Fig. 8, but for H_z polarization. The same conclusions can be drawn for H_z polarization as for E_z polarization: the combination of refractive index and radius disorder alone is sufficient to have almost the same effect on $\langle \ln T \rangle$ as the combined effects of five types of disorder. Such strong disorder again eliminates band gaps, as in the case of E_z polarization. Thus for the parameter ranges that we considered the effects of the positional, thickness, and sliding disorder is small compared to the contribution from the refractive index and radius disorder.

IV. LOCALIZATION OF WAVES IN RANDOM PHOTONIC CRYSTALS

Here we consider the localization of electromagnetic waves in disordered photonic crystals and we also investigate the homogenization properties of strongly disordered photonic crystals. When an electromagnetic wave propagates in a random medium, scattering can change the character of wave transport from propagation to localization [21]. One of the key parameters that characterizes localization phenomena is the localization length l^*:

$$\frac{l^*}{d} = -\lim_{N_L \to \infty} \frac{2N_L}{\langle \ln T \rangle}. \tag{2}$$

Here T is the transmittance of the stack, N_L is the number of layers in the stack, and $h_L=d$ is the thickness of each layer. The localization length l^* characterizes the decay length of waves in the disordered medium. In numerical calculations, a localization scaling length l is usually calculated using a finite value for N_L. It is shown in [23] that at long wavelengths l incorporates Anderson localization and attenuation due to Fabry-Perot reflections from the first and the last interfaces of the stack. As the number of layers increases, l tends to l^* [12].

Long wavelength waves cannot resolve the structure of the photonic crystal and one can replace the photonic crystal with an equivalent medium of constant refractive index (homogenization). In [12] we considered the transition from localization to homogenization when the average refractive index of the inclusions equals that of the background medium n_b. Here we consider the more difficult case in which the ratio of the average refractive index of cylinders to that of the background is $\overline{n}/n_b=3$, with $n_b=1$. Before investigating localization and homogenization phenomena for the complex case of multiple cylinders per unit cell it is important to understand these properties for the more straightforward case $N_c=1$, which we treat here. This transition from localization to homogenization in the long wavelength limit is considered below for both polarizations.

Localization of electromagnetic waves in highly disordered two-dimensional photonic crystals

A plane wave incident on a grating excites the orders of the grating with

$$\sin\theta_p = \sin\theta_i + \frac{\lambda}{d}p, \tag{3}$$

where p is an integer. For $\lambda/d>1$ there is only one propagating order ($p=0$). The scattering process is then determined by the symmetric $S_0^{\oplus}$ and antisymmetric $S_0^{\ominus}$ scattering matrices of the grating, which are the solutions of the scattering problem for von Neumann and Dirichlet boundary conditions, respectively (see [13] for details). For normal incidence, the symmetric $S_0^{\oplus}$ and antisymmetric $S_0^{\ominus}$ scattering matrices of the grating, for $p=0$, can be approximated as

$$S_0^{\oplus} = \exp(ikd) + \frac{2\exp(ikd/2)}{ikd}D_0^s, \tag{4}$$

$$S_0^{\ominus} = -\exp(ikd) + \frac{4\exp(ikd/2)}{ikd}D_1^a, \tag{5}$$

where

$$D_0^s = -\frac{2i\exp(ikd/2)}{S_0+iM_0}, \tag{6}$$

$$D_1^a = \frac{2i\exp(ikd/2)}{S_0+S_2+iM_1}. \tag{7}$$

Here the monopole D_0^s and dipole D_1^a coefficients are the solutions of the symmetric and antisymmetric Rayleigh identities (see [13] for details), and the boundary value coefficients M_0 and M_1 are given by

$$M_m^E = \frac{nJ_m'(nka)Y_m(ka) - J_m(nka)Y_m'(ka)}{nJ_m'(nka)J_m(ka) - J_m(nka)J_m'(ka)}, \tag{8}$$

$$M_m^H = \frac{J_m'(nka)Y_m(ka) - nJ_m(nka)Y_m'(ka)}{J_m'(nka)J_m(ka) - nJ_m(nka)J_m'(ka)}, \tag{9}$$

for E_z and H_z polarizations, respectively. Here $J_m(x)$ and $Y_m(x)$ are the mth order Bessel functions of the first and second kind. If $\lambda/d>1$, the lattice sums S_0 and S_2 can be approximated as

$$S_0 = \frac{2}{kd} - \frac{2i}{\pi}\ln\frac{\gamma kd}{4\pi} - \frac{i(kd)^2}{4\pi^3}, \tag{10}$$

$$S_2 = \frac{2}{kd} - \frac{4\pi i}{3(kd)^2} + \frac{i}{\pi} + \frac{i(kd)^2}{8\pi^3}, \tag{11}$$

where $\gamma=1.781$ is the Euler constant [22]. We have seen (Sec. III E) that disorder of the refractive indices and radii of cylinders have strong effects on the transmittance, and consequently on the localization properties (2), of waves for the set of parameters that we studied. Thus to study localization, we consider for now just the combination of these two disorders with

$$n = \overline{n} + Q_n\delta_1 = \overline{n}(1+Q\delta_1), \tag{12}$$

$$a/d = \overline{a} + Q_a\delta_2 = \overline{a}(1+Q\delta_2), \tag{13}$$

where δ_i are uniformly distributed random variables in the range $[-1,1]$, while Q is the amplitude of the disorders.

After substitution of Eqs. (6) and (7) into Eqs. (4) and (5), the reflection r_1^0 and transmission t_1^0 coefficients giving the amplitudes of the propagating orders of the grating can be written in the form

$$r_1^0 = \frac{S_0^{\oplus}+S_0^{\ominus}}{2} = -\frac{2e^{ikd}}{kd}\left[\frac{1}{S_0+iM_0} - \frac{2}{S_0+S_2+iM_1}\right], \tag{14}$$

$$t_1^0 = \frac{S_0^{\oplus}-S_0^{\ominus}}{2} = e^{ikd} - \frac{2e^{ikd}}{kd}\left[\frac{1}{S_0+iM_0} + \frac{2}{S_0+S_2+iM_1}\right]. \tag{15}$$

Note that the first term in the brackets in Eqs. (14) and (15) comes from the solution of the symmetric problem in the monopole approximation, while the second term is the dipole approximation of the solution of the antisymmetric problem. The quantities M_0 and M_1 in Eq. (15) are obtained from Eqs. (8) and (9), respectively, for E_z and H_z polarization. The localization scaling length (2) for one layer can be written in the form

$$\frac{l}{d} = -\frac{4}{\int_{-1}^{1}\int_{-1}^{1}\ln|t_1^0|\,\boldsymbol{d\delta}}, \tag{16}$$

where $t_1^0(Q)$ is given by Eq. (15) and $\boldsymbol{\delta}$ is a two-component vector $\boldsymbol{\delta}=(\delta_1,\delta_2)$. The transmission of a stack with two layers can be written as

$$t_{2L}(Q) = \frac{t_1^0 t_2^0}{1-r_1^0 r_2^0}, \tag{17}$$

where $r_i^0(Q)$ and $t_i^0(Q)$ $(i=1,2)$ are given by Eqs. (14) and (15). After substitution of Eq. (17) into Eq. (2), the localization length takes the form

$$\frac{l}{d} = -\frac{1}{\frac{1}{8}\int_{-1}^{1}\ln|t_1^0|\,\boldsymbol{d\delta}_1 - \frac{1}{32}\int_{-1}^{1}\int_{-1}^{1}\ln|1-r_1^0 r_2^0|\,\boldsymbol{d\delta}_1\boldsymbol{d\delta}_2}, \tag{18}$$

where $\boldsymbol{d\delta}$ are two-component vectors $\boldsymbol{d\delta}=(\delta_{1i},\delta_{2i})$. The expressions (16) and (18) are the general equations that we will use to describe the localization and homogenization for both polarizations.

1. Localization and homogenization for H_z polarization

In Fig. 10 we plot the localization length's dependence on wavelength for different numbers N_L of layers in the stack. We can see three distinct regions of behavior of l: a plateau region $\lambda<3.5d$, a transition region $3.5d<\lambda<5d$, and a long wavelength region $\lambda>5d$. It is seen that the localization length l for $N_L=100$ and $N_L=20$ layer stacks are nearly the same in the plateau and transition regions $\lambda<5d$. Thus edge effects are not important and states are truly localized. The sharp change in the localization length in the transition re-

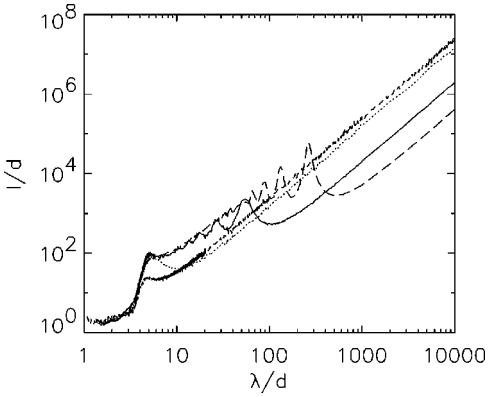

FIG. 10. Localization length versus wavelength for $N_L=100$ (long dashed line) and $N_L=20$ (solid line). The short dashed line represents the localization length behavior l based on Eq. (16), while the dotted line represents the localization length behavior based on Eq. (18). The degree of disorder is $Q=0.5$. Other parameters are given in the text.

gion can be viewed as defining the edge of a random gap. Thus the analytical description based on a single layer (16) (see Fig. 10, short dashed line) gives a qualitative agreement with the numerical simulations for multiple layers, while a calculation based on two layers (18) is in excellent agreement with the numerical calculation at short wavelengths. Since the one-layer model correctly predicts the position of the transition, it contains some of the essential physics of localization in this regime.

The localization length l is roughly the scale over which the constant of diffusion renormalizes to zero due to complete destructive interference. The renormalized diffusion coefficient $\overline{D}(\lambda)$ can be written in the form [21]

$$\overline{D}(\lambda)\approx D(\lambda)-\delta D(\lambda), \tag{19}$$

where $D(\lambda)$ is the diffusion coefficient and $\delta D(\lambda)$ is the renormalization correction due to scattering. These quantities for the two-dimensional case can be estimated as [21,24,25]

$$D(\lambda)\approx \frac{\lambda^3}{Q^2}, \tag{20}$$

$$\delta D(\lambda)\approx \lambda \ln(L\lambda^3), \tag{21}$$

where L is the sample size. The localization length l can be estimated from Eq. (19) by setting $\overline{D}(\lambda)=0$ and replacing L by localization length l. We obtain

$$\frac{l}{d}\sim c_1\frac{\lambda^3}{d^3}\exp(c_2\lambda^2/d^2), \tag{22}$$

where the coefficient $c_2\sim 1/Q^2$. This implies that a plot of $\ln(ld^2/\lambda^3)$ versus $(\lambda/d)^2$ should be a straight line. We test this in Fig. 11(a), in which our numerical results for six different Q values are redrawn in this way. Indeed, a linear dependence can be discerned for $6d<\lambda<25d$; best fits to a straight line are also indicated. In Fig. 11(b) we plot the slope c_2 of this linear dependence versus Q (solid line); error bars are included. For strong disorder ($Q>0.6$), c_2 scales as

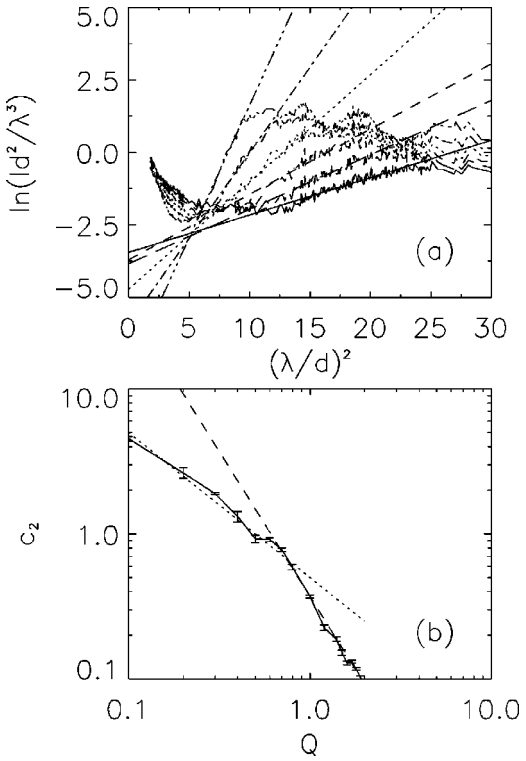

FIG. 11. (a) Localization length versus wavelength for different degrees of disorder for H_z polarization: $Q=0.6$ (dashed triple dot line), $Q=0.8$ (dashed dotted line), $Q=1.0$ (dotted line), $Q=1.2$ (dashed line), $Q=1.4$ (long dashed line), $Q=1.6$ (solid line). The region of the linear dependence of l on wavelength is in agreement with Eq. (22). (b) Slope c_2 of the linear dependence of the localization length l versus Q.

$c_2\approx 1/Q^2$ [dashed line in Fig. 11(b)] in agreement with Eq. (22). This is reminiscent of amorphous semiconductors in which the slope of Urbach tails are proportional to the mean-square displacement of atoms from their equilibrium positions [26]. For weak disorder ($Q<0.6$) the slope c_2 scales as $c_2\approx 1/Q$ [dotted line in Fig. 11(b)].

In the region $\lambda>5d$ in which waves cannot resolve the inclusions, the structure homogenizes. In [12] we found an expression for the effective dielectric constant ε_{eff} for weak randomness and multiple cylinders per unit cell. Here we calculate ε_{eff} for strong randomness. From Eq. (29) in [12] we deduce that for one cylinder per unit cell and for H_z polarization, ε_{eff} for one layer can be written as

$$\varepsilon_{\text{eff}}=1+\left\langle \frac{2f}{\dfrac{n^2+1}{n^2-1}-\dfrac{S_2}{\pi}f}\right\rangle, \tag{23}$$

where $f=\pi a^2/d^2$ is the filling fraction and the refractive indices n and radii a of cylinders are given by Eqs. (12) and (13). Here $S_2/\pi=\pi/3$ for a single layer and $S_2/\pi=1$ for an infinite stack. Numerically we observe that S_2/π tends to unity (i.e., not $\pi/3$) quickly as we increase the number of layers in the stack. Thus the homogenization is intrinsically two-dimensional for $N_L\geqslant 8$.

After averaging Eq. (23) and taking into account strong disorder, ε_{eff} takes the form for a single layer:

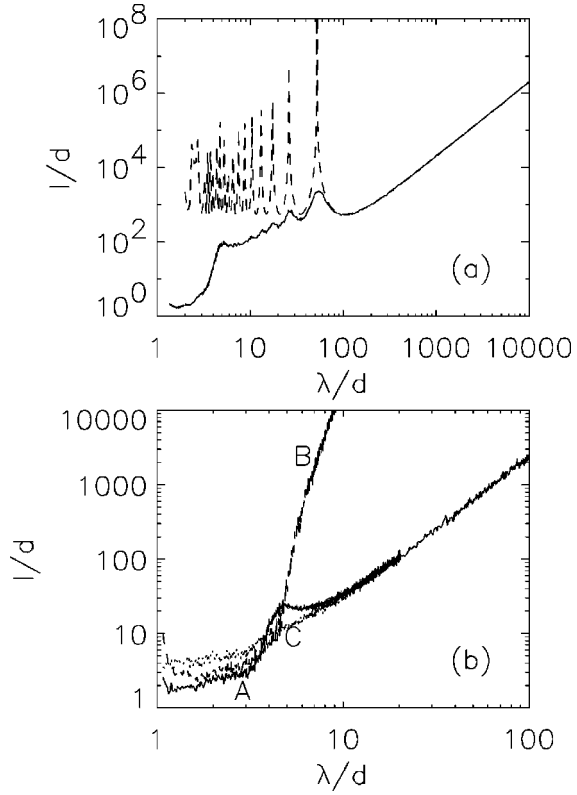

FIG. 12. (a) Dependence of l/d on λ/d (solid line) for H_z polarization. The dashed line is the inverse of the transmittance of a slab with effective dielectric constant ε_{eff} from Eq. (24) and thickness $N_L d$ with $N_L=20$. The degree of disorder is $Q=0.5$. (b) Localization length l versus wavelength λ for one layer $N_L=1$ calculated with both coefficients monopole D_0^s and dipole D_1^a (curve A). Curve B is the same quantity calculated with only the monopole coefficient D_0^s and curve C is calculated with only the dipole coefficient D_1^a.

$$\varepsilon_{\text{eff}}=1+\frac{2f}{\frac{\overline{n^2}+1}{\overline{n^2}-1}-\frac{\pi}{3}f}+\frac{2fQ^2}{3}\frac{\overline{n^4}(1+\pi f)+1-\pi f+\frac{2\pi}{3}f\overline{n^2}(3\overline{n^2}+1)}{(\overline{n^2}-1)^2\left[\frac{\overline{n^2}+1}{\overline{n^2}-1}-\frac{\pi}{3}f\right]^3}, \tag{24}$$

where $f=\pi\overline{a^2}/d^2$. In Fig. 12(a) (solid line), we plot localization length l versus wavelength for randomness $Q=0.5$ with $N_L=20$. The same quantity is also shown for a slab of a dielectric with ε_{eff} (dashed line). Good agreement between the two results implies that the random set of strongly disordered dielectric cylinders homogenizes to a dielectric slab with ε_{eff} given by Eq. (24) for $\lambda>60d$.

In Fig. 12(b) we plot l/d as a function of wavelength for one layer. The solid line (curve A) represents the localization length l calculated from Eq. (16) using Eq. (15), the dashed line (curve B) corresponds to the case in which we calculate l using only the dipole term (the second term) in Eq. (15), while the dotted line (curve C) represents l calculated using only the monopole solution D_0^a. It is seen that the homogenization properties for H_z polarization in the long wavelength region $\lambda/d>5$ are determined by the dipole coefficient D_1^a from Eq. (7) and, hence, by the solution of the antisymmetric problem. As the wavelength decreases, the term involving the monopole coefficient D_0^s from Eq. (6) becomes important and the localization properties are determined by both coefficients D_0^s and D_1^a. The changeover from localization to homogenization takes place at wavelengths for which $D_0^s\approx D_1^a$.

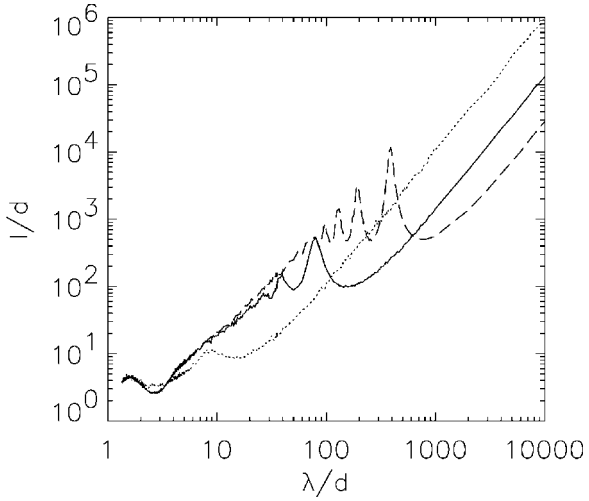

FIG. 13. The numerically determined localization length versus wavelength for $N_L=100$ (dashed line), $N_L=20$ (solid line) and the dotted line represents the localization length behavior l based on Eq. (18). The degree of disorder is $Q=0.5$. Other parameters are given in the text.

2. Localization and homogenization for E_z polarization

For E_z polarization we show that the localization properties for a stack with an arbitrary number of layers can be deduced from those for a stack with two layers ($N_L=2$) as will be seen below. In Fig. 13 we present numerical values of l/d versus wavelength for a stack with $N_L=100$ layers (short dashed line), $N_L=20$ layers (solid line), with the dotted line representing the analytical prediction based on Eq. (18). It is seen that the localization length l/d for wavelengths $1.3d<\lambda<10d$ does not depend on the number N_L of the layers in the stack. Thus waves with these wavelengths are localized. It is seen that the two-layer model based on Eq. (18) is in satisfactory agreement with the numerical calculation at $1.3d<\lambda<10d$.

In the limit of long wavelengths, the structure homogenizes. From Eq. (21) of [12] (see also [27]) and by taking into account Eqs. (12) and (13), the effective dielectric constant for a strongly disordered case for a single layer can be written as

$$\langle\varepsilon_{\text{eff}}\rangle=1+\langle f(n^2-1)\rangle=1+f\left(1+\frac{Q^2}{3}\right)\left[\overline{n^2}\left(1+\frac{Q^2}{3}\right)-1\right], \tag{25}$$

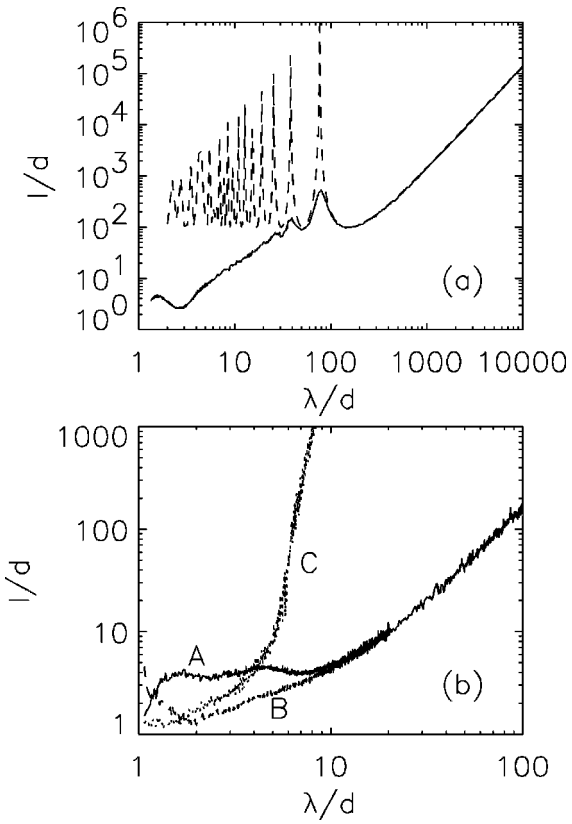

FIG. 14. Same as for Fig. 12, but for E_z polarization.

where $f=\pi\overline{a^2}/d^2$. In Fig. 14(a) we plot the inverse of $\langle \ln T\rangle$ as a function of wavelength (solid line). The dashed line represents the same quantity for a slab with ε_{eff} given by Eq. (25). We can see the good agreement between the two curves, which implies that the strongly disordered photonic crystal homogenizes to a slab with ε_{eff} for $\lambda > 60d$. Figure 14(b) is the same as in Fig. 12(b), but for E_z polarization. The homogenization properties for long wavelength are now determined by the monopole approximation given by D_0^s. As the wavelength decreases, the dipole coefficient D_1^a increases, leading to localization. This is the opposite of H_z polarization, in which the term D_1^a determines the homogenization and D_0^s sets in leading to localization. It is seen (see Fig. 13) that for E_z polarization we do not have a sharp transition from localization to homogenization at wavelengths $3d<\lambda<5d$, as for H_z polarization. Instead, the localization length increases gradually for $6d<\lambda<30d$. The localization length is only slightly dependent on N_L in this transition region.

V. CONCLUSION

We have studied the effects of the different types of disorder on the transmittance properties of two-dimensional photonic crystals composed of circular cylinders. The effects of the various types of disorder are

(1) *Refractive index disorder*. For small randomness, $\overline{n} \gg Q_n$ and E_z polarization, the refractive index disorder affects the longer wavelength part of the first photonic band gap. As we increase the number of the cylinders per unit cell the width of the gap reduces slightly. We observed slight oscillatory behavior of $\langle \ln T\rangle$ for E_z polarization and small randomness, while the H_z polarization is very sensitive to the randomness and even a small degree of randomness reduces the depth of the band gap (see [12] for details).

(2) *Radius disorder*. Even weak radius disorder induces resonances in the gap for the case of E_z polarization. This proves to be a whole-stack effect involving multiple reflections between first and last interfaces; it vanishes in the infinite-medium limit. As we increase the degree of disorder the band gaps fill in and eventually it becomes impossible to determine the position of the gaps from the transmission characteristics. In the case of H_z polarization $\langle \ln T\rangle$ is very sensitive to the degree of disorder. Even a small amount of disorder substantially increases $\langle \ln T\rangle$ in the band gaps.

(3) *Positional disorder*. Interestingly, positional disorder in the cylinders centers mainly affects the first gap for E_z polarization and has little effect on the second. Again, disorder induces the resonances in the first gap. The case of H_z polarization has similar characteristics to those seen for radius disorder: even a small amount of disorder has a strong effect on $\langle \ln T\rangle$, which is substantially increased in band gaps. Sliding disorder has the weakest effect on $\langle \ln T\rangle$, with the gap slightly deepening for both polarizations as the degree of the randomness is increased.

(4) *Thickness disorder*. Thickness disorder has a smoothing effect on $\langle \ln T\rangle$ for both polarizations, since the oscillatory behavior near the edges of the gaps is smeared out.

(5) *Combination of strong disorder*. By considering the disorder of all parameters at once we have seen that refractive index and radius disorders have the most effects on $\langle \ln T\rangle$ for both polarizations for the parameters considered. Strong disorder $Q_\xi \sim \overline{\xi}$ strongly effects $\langle \ln T\rangle$, and the information about the positions of the gaps is lost.

In summary, the resonance behavior of $\langle \ln T\rangle$ takes place for the case of E_z polarization and the radius, positional, and refractive index disorders, although for the latter case the oscillations are less pronounced (see [12]). All our calculations show that as we introduce a weak randomness of the refractive index, radius, or position of cylinders for E_z polarization, the randomness sets in at the longer wavelength part of the first gap through the resonancelike behavior of $\langle \ln T\rangle$.

The case of H_z polarization is very sensitive to the degree of disorder, whether we disorder refractive indices, radii, or positions. Even a small amount of disorder strongly affects the transmittance.

Localization properties have shown that waves for both polarizations are localized at wavelengths $1.3d<\lambda<5d$. An analytical description of the localization length has also been provided in terms of a quadrature. For H_z polarization it is shown that the slope of the exponential coefficient of the localization length is proportional to the inverse of the square of randomness (Q^{-2}) for strong disorder and proportional to (Q^{-1}) for weak disorder.

We have examined the transition from localization to homogenization that takes place for long wavelengths. We have

shown that it is governed by the interplay between monopole and dipole terms in the local potential expansions. The effective dielectric constants for strongly disordered photonic crystals have also been given for both polarizations. We also showed numerically that the homogenization of the strongly disordered photonic crystals is intrinsically two-dimensional, which indicates that the studied localization is also two-dimensional.

ACKNOWLEDGMENTS

The authors are grateful to P. Das for help in preparing the graphs and some of the computations. The Australian Research Council supported this work. Computer facilities at NSW Center for Parallel Computing were also provided by the ARC.

[1] E. Yablonovitch, Phys. Rev. Lett. **58**, 2059 (1987).
[2] S. John, Phys. Rev. Lett. **58**, 2486 (1987).
[3] *Photonic Band Gap Materials*, Vol. 315 of *NATO Advanced Study Institute, Series A*, edited by C.M. Soukoulis (Kluwer, Dordrecht, 1995).
[4] J.D. Joanopoulos, R.D. Meade, and J.N. Winn, *Photonic Crystals: Molding the Flow of Light* (Princeton University, Princeton, NJ, 1995). See also the special issue on photonic crystals in J. Lightwave Technol. **17**, 1928 (1999).
[5] J. Dowling, H. Everitt, and E. Yablonovitch, http://home.earthlink.net/~jpdowling/pbgbib.html.
[6] O. Painter, R.K. Lee, A. Scherer, A. Yariv, J.D. O'Brien, P.D. Dapkus, and I. Kim, Science **284**, 1819 (1999).
[7] B. Temelkuran, M. Bayindir, E. Ozbay, R. Biswas, M.M. Sigalas, G. Tuttle, and K.M. Ho, J. Appl. Phys. **87**, 603 (2000).
[8] J.C. Knight, J. Broeng, T.A. Birks, and P.St.J. Russel, Science **282**, 1476 (1998).
[9] K. Busch and S. John, Phys. Rev. Lett. **83**, 967 (1999).
[10] S. Fan, P.R. Villeneuve, and J.D. Joanopoulos, J. Appl. Phys. **78**, 1415 (1995).
[11] M.M. Sigalas, C.M. Soukoulis, C.-T. Chan, and D. Turner, Phys. Rev. B **53**, 8340 (1996).
[12] A.A. Asatryan, P.A. Robinson, L.C. Botten, R.C. McPhedran, N.A. Nicorovici, and C.M. de Sterke, Phys. Rev. E **60**, 6118 (1999).
[13] R.C. McPhedran, L.C. Botten, A.A. Asatryan, N.A. Nicorovici, P.A. Robinson, and C.M. de Sterke, Aust. J. Phys. **52**, 791 (1999).
[14] R.C. McPhedran, L.C. Botten, A.A. Asatryan, N.A. Nicorovici, P.A. Robinson, and C.M. de Sterke, Phys. Rev. E **60**, 7614 (1999).
[15] L.C. Botten, N.A. Nicorovici, A. A. Asatryan, R.C. McPhedran, P.A. Robinson, and C.M. de Sterke, J. Opt. Soc. Am B (to be published).
[16] S. John, Phys. Rev. Lett. **53**, 2169 (1984).
[17] S. John, Comments Condens. Matter Phys. **14**, 193 (1988).
[18] V.D. Freilikher and S.A. Gredeskul, Prog. Opt. **30**, 137 (1992).
[19] F. Urbach, Phys. Rev. **92**, 1324 (1953).
[20] M.C. Hutley, *Diffraction Gratings* (Academic, London, 1982).
[21] P. Sheng, *Introduction to Wave Scattering, Localization, and Mesoscopic Phenomena* (Academic, San Diego, 1995).
[22] V. Twersky, Arch. Ration. Mech. Anal. **8**, 323 (1963).
[23] L.C. Botten, C.M. de Sterke, R.C. McPhedran, N.A. Nicorovici, A.A. Asatryan, and P.A. Robinson (unpublished).
[24] S. John, in *Scattering and Localization of Classical Waves in Random Media*, edited by P. Sheng (World Scientific, Singapore, 1990).
[25] E. Abrahams, P.W. Anderson, D.C. Licciardello, and T.V. Ramakrishnan, Phys. Rev. Lett. **42**, 673 (1979).
[26] G.D. Cody, T. Tiedje, B. Abeles, B. Brooks, and Y. Goldstein, Phys. Rev. Lett. **47**, 1480 (1981).
[27] K. Busch and C.M. Soukoulis, Phys. Rev. B **54**, 893 (1996).